ACS Sustainable Resource Management

pubs.acs.org/acssrm

Article

Value-Added Lanthanum-Containing Products Recovered from Spent Cracking Catalyst

Inna Kozlovskaya,* Vladzimir Martsul, and Valentin Romanovski*

Cite This: *ACS Sustainable Resour. Manage.* 2024, 1, 2593−2601

Read Online

ACCESS | Metrics & More | Article Recommendations | Supporting Information

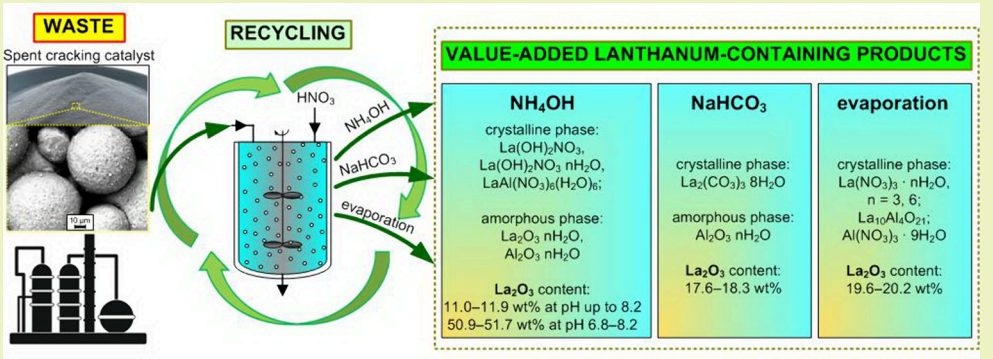

ABSTRACT: One of the wastes that can be considered as a promising secondary raw material is a spent catalyst for cracking petroleum hydrocarbons, containing up to 4 wt % rare earth elements. The work analyzes in detail three methods for recovering lanthanum from leaching solutions of spent catalytic cracking catalysts. Selective precipitation with ammonia solution in the pH ranges of 3.2−6.8 and 6.8−8.2 made it possible to partially separate aluminum and obtain products with a La_2O_3 content of 50.9−51.7 wt %. The sediments contain basic lanthanum salts and their hydrates, complex lanthanum and aluminum salts, and lanthanum and aluminum hydroxides. The La_2O_3 content in the precipitation product with a saturated solution of sodium bicarbonate in the pH range of 4.5−4.7 was 17.6−18.3 wt %. The precipitate is a mixture of hydrated lanthanum carbonate and aluminum hydroxide. As an alternative method for recovering lanthanum compounds, evaporation of a nitric acid leaching solution was considered. Evaporation does not require additional reagents and allows one to obtain a solution of nitric acid at a concentration of 10.8 M for reuse. The residue after evaporation contains at least 80.0 wt % of the liquid phase and after cooling to 30−35 °C is a mixture of hydrated aluminum and lanthanum nitrates. The lanthanum content in the solid residue after evaporation and heat treatment reaches 19.6−20.2 wt %.

KEYWORDS: *spent catalytic cracking catalyst, lanthanum, leaching, recovery*

1. INTRODUCTION

High rates of natural resource consumption lead to depletion, making waste reuse a valuable research area that aligns with UN Sustainable Development Goal 12.[1] Recycling conserves resources, as waste often contains higher valuable component levels than ore.[2−4] After extracting target substances from waste,[5−8] managing residual materials remains crucial.[9]

Spent zeolite-based sorbents and catalysts from gas drying, oil refining, and organic synthesis processes can serve as secondary raw materials. This includes spent catalysts for petroleum cracking, which contain rare earth elements (REEs) such as lanthanum (up to 4 wt %).[10] Annually, 400 thousand to 1 million tons of these catalysts are consumed, generating significant waste.[11,12] Extracting REEs from spent catalytic cracking catalysts (SCC) is thus promising.

REEs are used in petrochemistry, glass, ceramics, metallurgy, and electronics, with demand increasing due to the high-tech industries. Currently, REEs are obtained from minerals like bastnäsite, monazite, and xenotime, with REE oxide contents up to 75%.[13,14] Ores usually contain 5.0−9.0% REE oxides. REEs exist in these rocks as fluorocarbonates, phosphates, and complex salts with fluoride, chloride, and phosphate anions. Various wastes containing up to 1% REEs have been studied as secondary raw materials. However, extraction technologies for these are complex and produce large secondary waste volumes. In contrast, spent cracking catalysts have a simpler composition and higher REE content, making them a promising REE source. The main stages for extracting REEs

Received: September 11, 2024
Revised: November 22, 2024
Accepted: November 22, 2024
Published: November 27, 2024

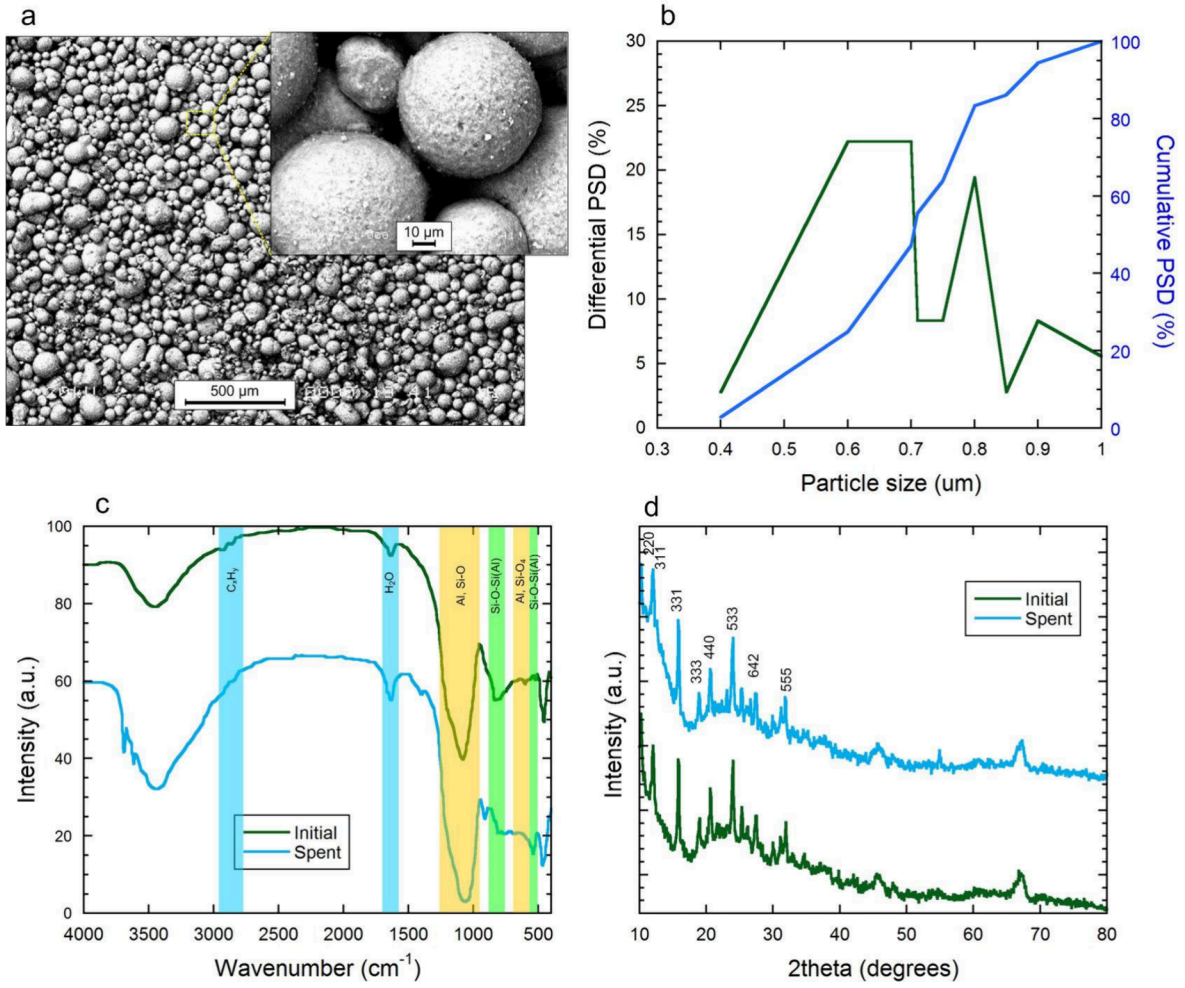

Figure 1. SEM image of SCC granules (a), PSD (b), IR spectra (c), and XRD of initial and spent SCC (d).

from waste or natural materials include leaching, REE recovery, and further refining to obtain pure elements. Acidic leaching, using mineral[15−17] and organic acids,[18,19] is standard. Bioleaching is also explored, though it often yields lower La recovery than inorganic acids.[20−22] Using HCl at 2 mol/L, a 1:10 solid-to-liquid ratio, and 60 °C for 2 h achieved 99.3% REE leaching efficiency after roasting at 750 °C.[23] Ce recovery from SCC using HCl with H_2O_2 reached 93%.[24] Combining HCl leaching with microwave treatment resulted in 99% La and Al recovery.[25] HCl was found to be more effective for La recovery (99.4%) compared to sulfuric acid.[26] Sulfuric acid leaching resulted in 85.6% La recovery,[11,27] while nitric acid achieved over 95%.[28]

The purpose of the work was to establish the patterns of recovery, composition, and properties of lanthanum-containing products obtained from acidic SCC leaching solutions. To achieve this goal, the following objectives were solved: (i) establish the chemical and phase composition physicochemical properties of the spent cracking catalyst, which determine the possibility and direction of its use as a raw material for the production of rare earth elements; (ii) justify and experimentally test methods for recovery of lanthanum-containing products from leaching solutions of spent petroleum hydrocarbon cracking catalyst; (iii) investigate the chemical and phase composition of lanthanum-containing products and determine the areas of their application; and (iv) develop technological schemes of proposed methods for recovery of lanthanum-containing products from leaching solutions.

2. MATERIALS AND METHODS

2.1. Reagents. Spent petroleum hydrocarbon cracking catalyst was collected from an oil refinery. The true density of SCC is 1.78 g/mL, and the bulk density varies for different batches from 0.8 to 1.1 g/mL. A more detailed analysis of the SCC is presented in Subsection 3.1.

Chloroform and methanol were used to assess the residual content of organic substances in SCC by using gas chromatography−mass spectrometry.

A 25% ammonia solution and a saturated sodium carbonate solution were used to precipitate lanthanum-containing products from acid leaching solutions. Solutions of sulfuric and nitric acids were used for leaching.

2.2. Recycling of SCC. One-factor experiments on acid leaching of lanthanum were carried out at a mass ratio of SCC to a solution of nitric or sulfuric acid equal to 1:10 according to ref 29. The effect of temperature on the degree of acid leaching was studied in the range of 20−90 °C. The range of concentrations of nitric acid solutions studied was 4−14 mol/L and of sulfuric acid was 3−18 mol/L. The duration of the leaching process is 0.5−4 h.

Recovery of lanthanum compounds from acidic leaching solutions was carried out in three ways: (i) precipitation with a 25 wt % ammonia solution, (ii) precipitation with a saturated solution of sodium bicarbonate, and (iii) evaporation of nitrate concentrate.

Recovery of lanthanum compounds from acidic leaching solutions by precipitation with a 25% ammonia solution was carried out until a

https://doi.org/10.1021/acssusresmgt.4c00364
ACS Sustainable Resour. Manage. 2024, 1, 2593−2601

pH value of 8.2 was reached, during which coprecipitation of aluminum hydroxide and lanthanum occurs.

To precipitate lanthanum compounds from leaching solutions in the form of carbonates, a saturated solution of sodium bicarbonate was used.

Recovery of lanthanum compounds from a nitric acid leaching solution by evaporation was carried out at the temperature of formation of the azeotropic mixture (121.9 °C). At least 80.0% of the initial volume of the solution was evaporated, while in the Al^{3+}–La^{3+}–HNO_3–H_2O system the concentration of dissolved salts increases, which leads to supersaturation of the solution and to the formation of nuclei of aluminum nitrate crystals. Complete crystallization of the residue occurred when the temperature was decreased to 30–35 °C.

2.3. Methods of Sample Analysis. The study of physicochemical properties and identification of the chemical and phase composition of SCC and its processing products was carried out using electron scanning microscopy and X-ray fluorescence analysis (scanning electron microscope JSM 5610 LV with an elemental analysis system EDX JED 2201 JEOL, equipped with an X-ray fluorescence analysis system, measured concentration range 0.1–100%); X-ray phase analysis (D8 ADVANCE diffractometer from Bruker with a step-by-step shooting method, with a step of 0.03° along the 2θ angle and a shutter speed at each point of 3 s in the angle range 20–80° θ); thermogravimetric analysis (TG, DTG) and differential scanning calorimetry (TGA/DSC derivatograph from Mettler Toledo up to a maximum temperature of 800 °C using Al_2O_3 as a standard; platinum crucibles; heating rate, 10 °C/min; sample weight, 60.3–60.9 mg); a low-temperature method for nitrogen adsorption–desorption (NOVA 2200 device, determination range from 10 to 1000 m^2/g, measurement principle based on the BET method); and atomic absorption spectrometry (Avanta atomic absorption spectrometer with a graphite furnace System 3000) to determine microimpurities of metals. pH determination was carried out on a HANNA HI 221 pH meter with a combined glass electrode HI 1131P (measurement error 0.01 pH).

To process the experimental results, the software of the corresponding devices was used. The number of parallel samples is at least three.

3. RESULTS AND DISCUSSION

3.1. Characterization of SCC. SCC, a fine gray powder with spherical granules (Figures 1a and 1b), has particle sizes ranging from 5–100 μm, following a normal distribution. According to IR spectroscopy (Figure 1c) and X-ray phase analysis (Figure 1d), the zeolite crystal structure in SCC matches that of synthetic type Y zeolite, which remains stable during catalyst use.

The IR spectrum of SCC resembles that of zeolite Y,[30] with absorption bands at 200–1300 cm^{-1} linked to the vibrations of Al and Si–O_4 tetrahedra in the zeolite framework. Key bands at 950–1250, 720–650, and 420–500 cm^{-1} indicate stretching and bending within the zeolite tetrahedra, while bands at 500–600 and 300–420 cm^{-1} suggest vibrations in the external bonds and entrance rings of the zeolite structure. Bands in the 3400–3500 cm^{-1} range correspond to hydroxyl group vibrations, while the 1637 cm^{-1} band is due to the bending of water adsorbed on the zeolite. Hydrocarbon presence, indicated by bands at 2800–2900 cm^{-1}, may include polycyclic aromatic hydrocarbons due to the catalyst's regeneration conditions (up to 800 °C with oxygen).

Table 1 presents SCC composition data for samples with a variable lanthanum content. Heavy metals (lead, chromium, cobalt) are below 0.003%, cadmium is up to 0.0007%, iron is up to 0.30%, and zinc and nickel are between 0.050–0.090%. Sodium content results from the NaY zeolite were used in SCC production.

Table 1. Chemical Composition of SCC, wt %

	initial		spent	
element	elements	oxides	elements	oxides
O	49.0 ± 0.3	–	49.2 ± 0.3	–
Al	27.3 ± 0.3	51.6 ± 0.3	27.0 ± 0.3	51.1 ± 0.3
Si	21.2 ± 0.3	45.4 ± 0.3	21.1 ± 0.3	45.6 ± 0.3
La	1.8 ± 0.3	2.1 ± 0.3	1.5 ± 0.3	1.8 ± 0.3
Na	0.6 ± 0.3	0.9 ± 0.3	1.1 ± 0.3	1.5 ± 0.3

Chromatography–mass spectrometry of SCC's organic extract (chloroform–methanol) revealed no organic compounds due to high temperatures (450–750 °C) during cracking and regeneration. BET analysis shows an SCC-specific surface area of 89 m^2/g and a pore volume of 0.60 cm^3/g, reduced by 2.1–2.3 and 1.4–1.6 times from the original catalyst, respectively, indicating structural changes that complicate lanthanum extraction (IVa type of isotherms,[31] Figure 2).

3.2. Recovery of Lanthanum Compounds from Acid Solutions. *3.2.1. Acid Leaching of Lanthanum from SCC.* The primary factors influencing REE leaching from natural and waste materials include the leaching agent concentration, process duration, and temperature. These variables were selected based on prior data on REE extraction and single-factor experiments. Under identical conditions, lanthanum leaching rates differ significantly when sulfuric acid is used versus nitric acid (Figure 3).

The lanthanum leaching efficiency shows a complex relationship with acid concentration as increasing acid concentration lowers the solubility of lanthanum nitrate and sulfate. Temperature impacts leaching differently for each acid: with nitric acid, higher temperatures increase lanthanum solubility, whereas with sulfuric acid, lanthanum solubility decreases at elevated temperatures. This is because the lanthanum nitrate solubility increases with temperature, while lanthanum sulfate exhibits a negative temperature solubility coefficient.

For treatment time, lanthanum leaching with nitric acid increases linearly over 0.5–1.5 h and with sulfuric acid over 0.5–2.5 h. Extending the nitric acid treatment to 3 h improves leaching by 9.5%, and with sulfuric acid by 4.5%, making 3 h the practical limit for treatment.

The effects of the factors are varied, necessitating a series of three-level experiments to determine optimal conditions. The intervals for factor variations were set within the accuracy of the measurement. Data from single-factor experiments align with multi-factorial experiment results (Tables S1 and S2). Optimal conditions for lanthanum leaching were achieved with a 7 M nitric acid solution at 90 °C for 180 min, which was used in further studies.

During the extended test matrix of one-factor experiments, the dependence of the degree of acid leaching of lanthanum (LE) on the concentration of nitric acid solution (C, mol/L), treatment temperature (T, °C), and duration of the process (t, hours) was established (Table S2).

$$\mathrm{LE}\ (HNO_3) = -12.3642 + 19.2613 \cdot C + 0.2684 \cdot T - 2.1556 \cdot t + C \cdot t - 1.2782 \cdot C^2 - 0.4056 \cdot t^2$$

The calculated Student, Fisher, and Cochran tests confirm the adequacy of the chosen regression equation (Table S2).

https://doi.org/10.1021/acssusresmgt.4c00364
ACS Sustainable Resour. Manage. 2024, 1, 2593–2601

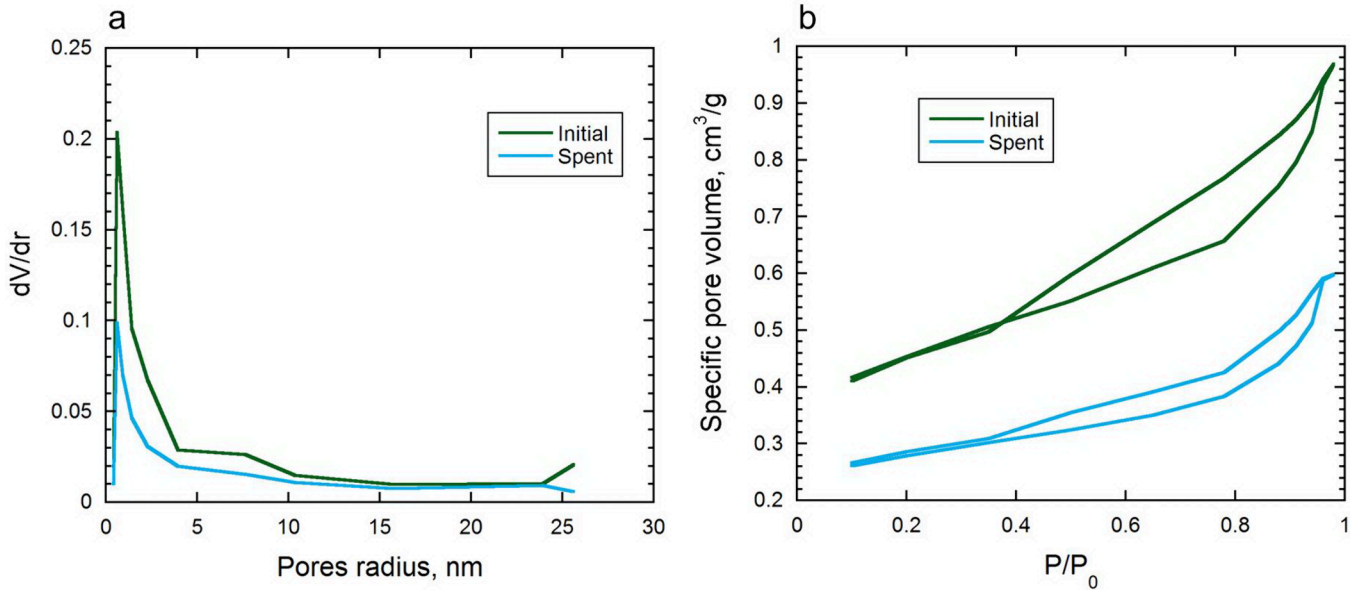

Figure 2. Differential mesopore size distributions in linear form (a) and isotherms of low-temperature nitrogen adsorption−desorption (b).

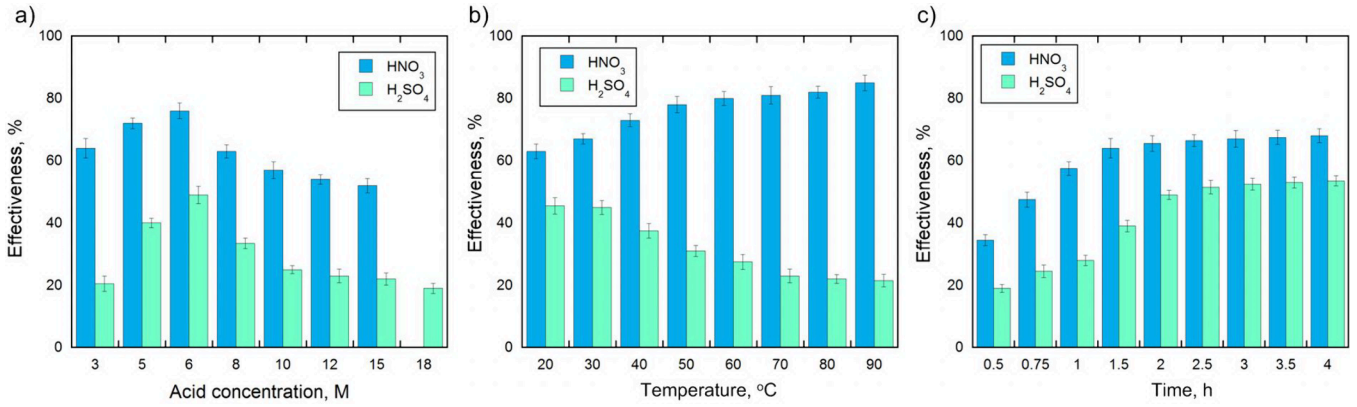

Figure 3. Dependence of the degree of lanthanum leaching from SCC with solutions of nitric and sulfuric acid on (a) the concentration of the acid solution (at 20 °C, 120 min), (b) the temperature (at an acid concentration of 7 M, 120 min), and (c) the leaching kinetics (at an acid concentration of 7 M and a temperature of 20 °C).

3.2.2. Recovery of Lanthanum Compounds from Nitric Acid Leaching Solutions by 25% Ammonia Solution. When an ammonia solution is used as a precipitant, lanthanum is released from solutions mainly in the form of hydroxy compounds. Lanthanum hydroxide precipitates as an amorphous, bulky sediment in the pH range of 7.28−8.16 (solubility product 1×10^{-19}−0.9×10^{-22}). In the presence of aluminum, coprecipitation of lanthanum hydroxide with aluminum hydroxide occurs (precipitation of aluminum hydroxide predominantly occurs in the pH range of 3.5−5.2 and ends at pH 7.2−7.6, solubility product 5×10^{-33}). The reactions occurring in the La^{3+}−Al^{3+}−NO_3^- system are as follows:

$$La^{3+} + 3OH^- + nH_2O \rightarrow La(OH)_3 \cdot nH_2O$$

$$La^{3+} + 2OH^- + NO_3^- + nH_2O \rightarrow La(OH)_2NO_3 \cdot nH_2O$$

$$La^{3+} + 2OH^- + NO_3^- \rightarrow La(OH)_2NO_3$$

$$La^{3+} + Al^{3+} + 6NO_3^- + 6H_2O \rightarrow LaAl(NO_3)_6(H_2O)_6$$

After thermal decomposition:

$$La(OH)_3 \cdot nH_2O \rightarrow La_2O_3 + nH_2O$$

$$La(OH)_2NO_3 \cdot nH_2O \rightarrow La_2O_3 + NO_2 + nH_2O$$

$$La(OH)_2NO_3 \rightarrow La_2O_3 + NO_2 + nH_2O$$

$$LaAl(NO_3)_6(H_2O)_6 \rightarrow La_2O_3 + Al_2O_3 + NO_2 + nH_2O$$

Experimental studies found that raising the pH to 8.2 with ammonia allows 95.0−99.0% of the lanthanum and aluminum to precipitate from the leaching solution. The initial concentrations were 1.8 g/L for lanthanum and 5.3 g/L for aluminum, reducing to 0.1−0.01 g/L for lanthanum and 0.27−0.05 g/L for aluminum after precipitation.

Elemental analysis indicated that the lanthanum content in sediments (as oxides) from nitric acid solutions at pH 8.2 reached 11.0% to 11.9% of the dry matter, 5.5 to 10.0 times higher than in SCC. The aluminum-to-lanthanum oxide mass ratio ranged from 4.9 to 7.7, with impurity levels (iron, copper, nickel) under 2%.

Selective precipitation with a 25% ammonia solution in the pH range 3.2−6.8 precipitated 80−85% of aluminum

https://doi.org/10.1021/acssusresmgt.4c00364
ACS Sustainable Resour. Manage. 2024, 1, 2593−2601

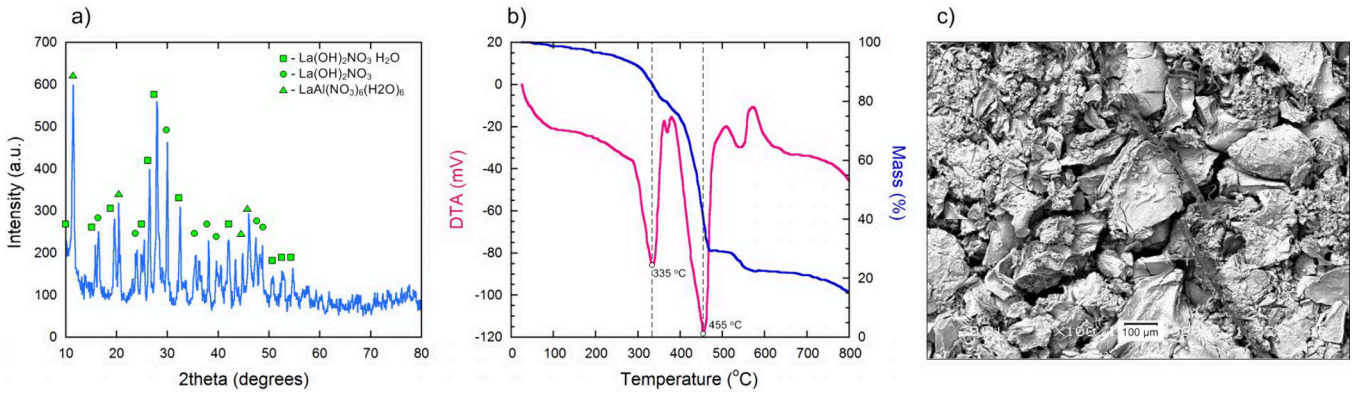

Figure 4. X-ray diffraction pattern (a), mass loss and DTA (b), and SEM image (c) of the precipitate obtained by precipitation from a nitrate solution with a 25% ammonia solution to pH 8.2.

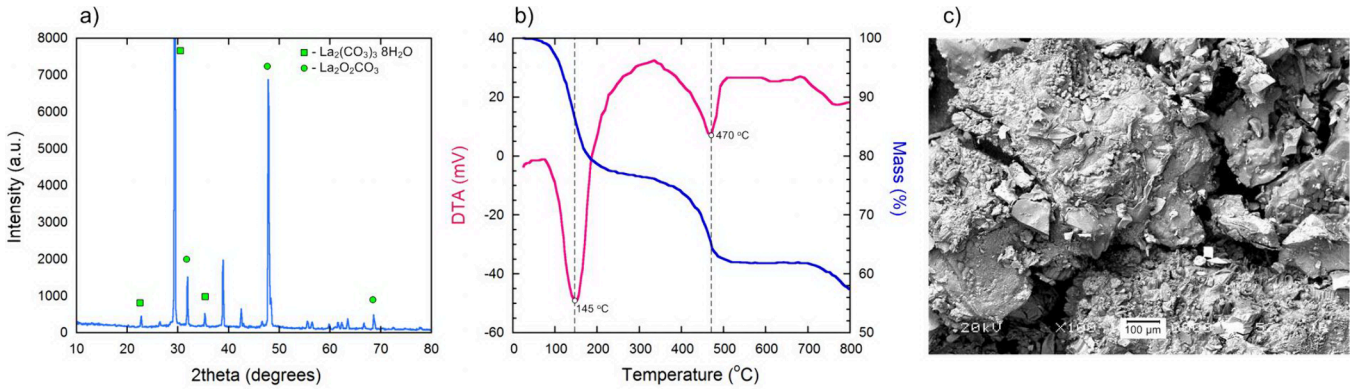

Figure 5. X-ray diffraction pattern (a), mass loss and DTA (b), and SEM image (c) of the precipitate obtained by precipitation with sodium bicarbonate.

hydroxide (residual Al concentration: 1.1−0.8 g/L). Between pH 6.8 and 8.2, up to 85.0% of lanthanum precipitated (final concentration <0.01 g/L). Lanthanum content in these sediments reached 50.9−51.7%, with an Al oxide ratio of 0.2−0.7 and impurities below 2%.

Sediments from SCC leaching contain amorphous and crystalline phases, including lanthanum dihydroxonitrate and its hydrate ($La(OH)_2NO_3$, $La(OH)_2NO_3{\cdot}H_2O$) and lanthanum−aluminum hexahydronitrate ($LaAl(NO_3)_6(H_2O)_6$) (Figure 4a). The amorphous phase likely consists of aluminum and lanthanum hydroxides. Hydrated compounds in the sediments are thermally unstable, with aluminum decomposing first, while lanthanum decomposes above 350 °C.

A thermogram (Figure 4b) of the sediment from nitric acid leaching (fractionally precipitated with ammonia and dried at 105 °C) shows three main endothermic peaks (Figure 4b). The first peak at 265−351 °C (maximum 335 °C) reflects the decomposition of aluminum hydroxide and main salts, with a 17.6 wt % mass loss (calculated: 34.0 wt %). Differences are due to partial water retention and possible formation of hydrated lanthanum compounds (Figure 4c). The second peak, at 380−480 °C (maximum 455 °C), corresponds to $LaAl(NO_3)_6(H_2O)_6$ decomposition, with a 59.2% mass loss (calculated: 55.4%). The third peak, at 504−567 °C (maximum 513 °C), indicates lanthanum hydroxo-compound decomposition, with a mass loss of 14.1% (calculated: 14.3%).

3.2.3. Recovery of Lanthanum Compounds from Acidic Leaching Solutions with Saturated Sodium Bicarbonate Solution. According to ref 32, when using carbonate solutions, complete precipitation of lanthanum compounds is achieved at a molar ratio of CO_3^{2-}:La = 1.5. Lanthanum carbonate precipitates as amorphous $La_2(CO_3)_3{\cdot}nH_2O$ in a pH range of 4.7−5.6, later transitioning to a crystalline form. Its solubility in sodium carbonate solution is 0.01−0.04 g/L (as La_2O_3).

In this study, lanthanum precipitation with a saturated carbonate solution was achieved at pH 4.5−4.7, yielding a 95.0−97.0% precipitation rate (residual La concentration: 0.1−0.05 g/L). When the pH was adjusted to 4.7, lanthanum precipitated as a hydroxide, with 57.5 wt % aluminum remaining in the solution (Al concentration: 2.0−2.3 g/L). Elemental analysis showed that the Al to La mass ratio in sediments from nitric acid solutions using sodium bicarbonate varied from 2.4 to 4.6. Lanthanum content in dried residues reached 17.6−18.3%, higher than that in the original catalyst (8.8−16.6%).

X-ray phase analysis (Figure 5a) indicated that sediments include amorphous $La_2(CO_3)_3$ and crystalline $La_2(CO_3)_3{\cdot}8H_2O$, with various hydrate forms, plus $La_2O_2CO_3$, but no crystalline aluminum phases.

The sediment's thermogram (Figure 5b) shows endothermic peaks at 145 °C (20.2% weight loss) and 470 °C (11.8% loss), likely due to dehydration and oxide formation from lanthanum carbonate. Differences in the values likely reflect aluminum compounds in the sediment (Figure 5c). The DTG curve at 180−207 °C shows decomposition of amorphous aluminum hydroxide to oxide.[33]

When carbonate solutions were used, complete precipitation of lanthanum compounds was achieved at a molar ratio of

https://doi.org/10.1021/acssusresmgt.4c00364
ACS Sustainable Resour. Manage. 2024, 1, 2593−2601

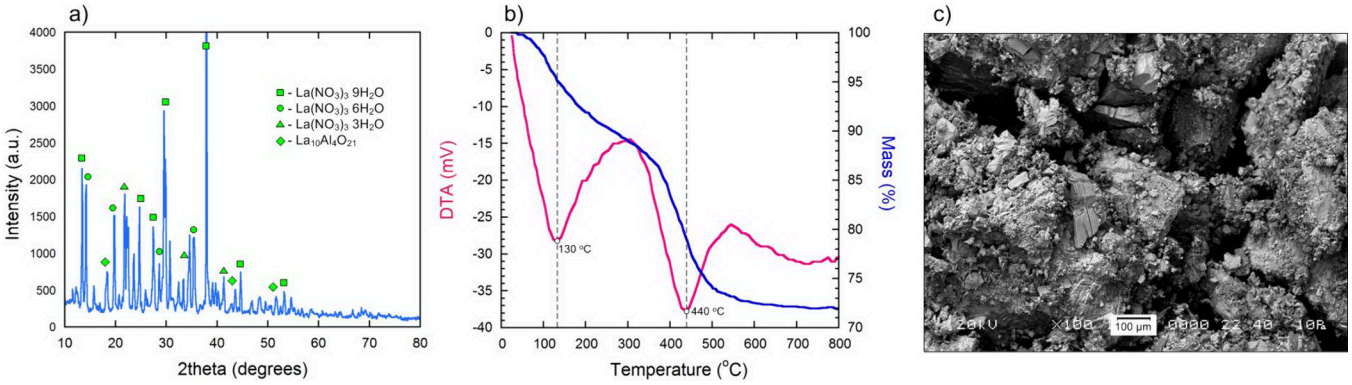

Figure 6. X-ray diffraction pattern (a), mass loss and DTA (b), and SEM image (c) of the residue after evaporation of the nitrate solution of SCC leaching.

Table 2. Composition of Lanthanum-Containing Products from Nitric Acid Leaching Solutions of SCC

selection approach	lanthanum content (in terms of La_2O_3), %	composition
precipitation with 25% ammonia solution at pH up to 8.2	11.0−11.9	crystalline phase, $La(OH)_2NO_3$, $La(OH)_2NO_3{\cdot}nH_2O$, $LaAl(NO_3)_6(H_2O)_6$; amorphous phase, $La_2O_3{\cdot}nH_2O$, $Al_2O_3{\cdot}nH_2O$
precipitation with 25% ammonia solution at pH 6.8−8.2	50.9−51.7	crystalline phase, $La(OH)_2NO_3$, $La(OH)_2NO_3{\cdot}nH_2O$, $La(OH)_3$; amorphous phase, $La_2O_3{\cdot}nH_2O$, $Al_2O_3{\cdot}nH_2O$
precipitation with sodium bicarbonate	17.6−18.3	crystalline phase, $La_2(CO_3)_3{\cdot}8H_2O$; amorphous phase, $Al_2O_3{\cdot}nH_2O$
evaporation	19.6−20.2	crystalline phase, $La(NO_3)_3{\cdot}nH_2O$ (n = 3, 6), $La_{10}Al_4O_{21}$, $Al(NO_3)_3{\cdot}9H_2O$

CO_3^{2-}:La = 1.5. REE carbonates are released in the form of amorphous precipitates of the composition $La_2(CO_3)_3{\cdot}nH_2O$ (pH 4.7−5.6), which over time transform into crystalline.

$$2La^{3+} + 3CO_3^{2-} + nH_2O \rightarrow La_2(CO_3)_3{\cdot}nH_2O$$

$$2La^{3+} + CO_3^{2-} + 2H_2O \rightarrow La_2O_2CO_3 + 4H^+$$

After thermal decomposition:

$$La_2(CO_3)_3{\cdot}nH_2O \rightarrow La_2O_3 + H_2O + CO_2$$

3.2.4. Recovery of Lanthanum Compounds from Acid Leaching Solutions by Evaporation of Nitrate Concentrate. Evaporation of a nitric acid leaching solution leverages nitric acid's boiling point of 82.6 °C, allowing removal without decomposition up to 121.9 °C (Figure 6b). This leaves lanthanum in the solid phase without additional reagents (Figure 6c), and the aluminum present does not hinder subsequent applications, although corrosion-resistant equipment is required.

Evaporating 80% of the SCC nitrate solution increases the salt concentration, leading to aluminum nitrate crystal formation due to the limited solubility of $Al(NO_3)_3$ in 7 mol/L nitric acid (73.9 g/100 mL), while lanthanum nitrate (75 g/100 mL) does not crystallize under these conditions (Figure 6a). Complete crystallization occurs as the temperature drops to 30−35 °C.

The solid residue melts between 39.8 and 76.7 °C, corresponding to the melting points of lanthanum and aluminum nitrate hydrates, confirmed by X-ray phase analysis (Figure 6a). Elemental analysis reveals an Al_2O_3 to La_2O_3 ratio of 4.1−4.9, with lanthanum content reaching 19.6−20.2% after heat treatment, up to 20 times higher than in SCC.

Thermogravimetric analysis shows distinct thermal stabilities (Figure 6b): aluminum nanohydrate decomposes to $Al(OH)_2NO_3{\cdot}1.5H_2O$ at 135 °C and to aluminum oxide at 200 °C. Lanthanum nitrate hydrates dehydrate at 240 °C and decompose to $LaONO_3$ at 515 °C. The residue's thermogram reveals two endothermic peaks: the first at 130 °C (10.1% mass loss) for dehydration and aluminum nitrate decomposition and the second at 450 °C (17.0% mass loss) for lanthanum nitrate decomposition.

Evaporation also enables nitric acid recovery without extra reagents. Between 107 and 115 °C, the solution reaches a nitric acid concentration of 2.1 and 5.6 mol/L, and at 119 °C, it reaches 10.8 mol/L.

When evaporated, the residue mainly contains hydrated aluminum and lanthanum nitrates, including $La(NO_3)_3{\cdot}3H_2O$, $La(NO_3)_3{\cdot}6H_2O$, and aluminum in the form of crystalline $Al(NO_3)_3{\cdot}9H_2O$. After thermal decomposition:

$$La(NO_3)_3{\cdot}3H_2O \rightarrow La_2O_3 + H_2O + NO_2$$

$$Al(NO_3)_3{\cdot}9H_2O \rightarrow Al_2O_3 + H_2O + NO_2$$

$$La_{10}Al_4O_{21} \rightarrow Al_2O_3 + La_2O_3$$

3.3. Analysis of the Possibility of Using the Resulting Products. Studies on various methods for leaching and recovering lanthanum from spent cracking catalysts (SCC) show that different process conditions yield products with lanthanum concentrations between 11.0% and 51.7%. Table 2 summarizes the composition of lanthanum-containing products (La_2O_3 content on a dry basis).

Most compounds in the resulting precipitates decompose at high temperatures, allowing dehydration through controlled thermal treatment. The lanthanum product from SCC can be used to produce lanthanum aluminate ($LaAlO_3$), applicable in refractories,[34] catalysts,[35] and phosphors.[36] Additionally, ceramics based on lanthanum hexaaluminate, which offers high hardness and mechanical strength, are valuable for functional materials and composites.[37]

The composition of the lanthanum product obtained after nitric acid evaporation aligns with the TU ST TOO 38960949-002-2006 requirements for "Nitrate Solution of Rare Earth

https://doi.org/10.1021/acssusresmgt.4c00364
ACS Sustainable Resour. Manage. 2024, 1, 2593−2601

Elements", supporting its use in zeolite-containing cracking catalysts. This grade B nitrate solution requires a minimum lanthanum concentration of 65 g/L, with impurity limits on iron (≤0.01%) and alkali metals (≤3.0%). The presence of aluminum is acceptable as the synthesis of zeolite catalysts involves aluminosilicate raw materials.

The lanthanum-containing product precipitated at pH 8.2 also meets the TU 14-5-136-81 standard for the FS30RZM5-15 alloy, which requires a rare earth element concentration between 5% and 15%, matching the lanthanum levels in the SCC-derived products.

Lanthanum-containing products from SCC can be considered as intermediates. It is possible to use them as raw materials for the production of high-purity lanthanum compounds using known technologies.[38] Compared with natural raw materials and known methods for obtaining REE from waste (the main stages include grinding → acid decomposition → leaching with water → diluting the solution → heating to boiling and neutralization with ammonia in different pH ranges → alkali treatment → dissolving hydroxides in nitric acid → extraction separation rare earth compounds), the number of stages in the recovery of lanthanum compounds is reduced (main stages include dosing of a neutralizing reagent (precipitant) → separation of the resulting precipitate → mechanical dehydration → washing and heat treatment of the precipitate).

Our study highlights the efficient recovery of lanthanum from spent catalyst components (SCC) through acid leaching, achieving up to 99% recovery with 7 M nitric acid at 90 °C. This approach proves effective compared to bioleaching with *Aspergillus niger*,[39,40] which reaches only 63% recovery at lower pulp densities due to inhibitory effects at higher concentrations and for nickel and vanadium bioleaching.[41−43] Chemical and structural analyses show that SCC's stable aluminosilicate matrix and Y-type zeolite structures facilitate lanthanum retention, favoring acid leaching over microbial methods.

Among the methods evaluated, nitric acid evaporation stands out for its scalability, environmental sustainability, and cost-effectiveness. It minimizes secondary waste through closed-loop acid recycling, meeting sustainability goals (SDG 12). Ammonia and sodium bicarbonate precipitation methods, while effective, generate substantial waste byproducts and require additional processing. Our results suggest that nitric acid evaporation, with its reduced reagent demand and waste output, offers significant advantages for industrial applications. This method yields high-purity La_2O_3 suitable for high-tech uses, such as in electronics and catalysts.[44−48] Future research should focus on optimizing energy consumption[49−51] and exploring alternative leaching agents to enhance the sustainability of lanthanum recovery from industrial waste.

4. CONCLUSIONS

The chemical and phase compositions of the spent cracking catalyst have been identified, suggesting its potential as a raw material for rare earth element production. Analysis shows the catalyst is a composite aluminosilicate with 2.1 ± 0.1 wt % La_2O_3, primarily composed of Y-type zeolite, whose structure remains stable with use. Microimpurities are at levels comparable to those of natural aluminosilicates.

Experiments indicate that lanthanum can be recovered from nitric acid leaching solutions of the catalyst by precipitation with 25% ammonia. Ammonia precipitation in pH ranges of 3.2−6.8 and 6.8−8.2 selectively removes aluminum, yielding products with 50.9−51.7 wt % La_2O_3. Precipitation at pH 8.2 yields products with 11.0−11.9 wt % La_2O_3, containing basic lanthanum salts, hydrates, and mixed lanthanum−aluminum compounds.

Lanthanum can also be recovered by precipitation with saturated sodium bicarbonate at pH 4.5−4.7, producing 17.6−18.3 wt % La_2O_3 as hydrated lanthanum carbonate alongside aluminum hydroxide.

An alternative method involves evaporating the nitric acid leaching solution, producing a reusable 10.8 mol/L nitric acid solution without extra reagents. The evaporated residue contains hydrated aluminum and lanthanum nitrates, with a solid lanthanum concentration of 19.6−20.2 wt % after heat treatment.

Lanthanum products from these processes can be used in refractory production, thermally resistant ceramics, cracking catalysts as a rare earth replacement, and in producing alloys such as FS30RZM5 according to TU 14-5-136-81 standards.

■ ASSOCIATED CONTENT

Data Availability Statement

All data, models, and code generated or used during the study appear in the submitted article.

Supporting Information

The Supporting Information is available free of charge at https://pubs.acs.org/doi/10.1021/acssusresmgt.4c00364.

Detailed tables (S1−S5) and figures (S1 and S2) to supplement the main manuscript, presenting data on lanthanum leaching efficiency, mass balances for different recovery methods, and process schematics, and additional text elaborating on experimental conditions, recovery methods (ammonia precipitation, sodium bicarbonate precipitation, and nitric acid evaporation), material flows, and scalability evaluations, offering a comprehensive understanding of the studied processes (PDF)

■ AUTHOR INFORMATION

Corresponding Authors

Inna Kozlovskaya − *Department of Industrial Ecology, Belarusian State Technological University, Minsk 220006, Belarus*; Email: kozlovskayainnay@gmail.com

Valentin Romanovski − *Department of Materials Science and Engineering, University of Virginia, Charlottesville, Virginia 22904, United States*; orcid.org/0000-0003-1741-0316; Email: rvd9ar@virginia.edu

Author

Vladzimir Martsul − *Department of Industrial Ecology, Belarusian State Technological University, Minsk 220006, Belarus*

Complete contact information is available at: https://pubs.acs.org/10.1021/acssusresmgt.4c00364

Author Contributions

I.K.: formal analysis, data curation, validation, investigation, methodology, visualization, writing−original draft, and writing−review and editing. V.M.: conceptualization, supervision, methodology, resources, data curation, validation, and writing−review and editing. V.R.: formal analysis, data curation, visualization, writing−original draft, and writing−review and editing.

https://doi.org/10.1021/acssusresmgt.4c00364
ACS Sustainable Resour. Manage. 2024, 1, 2593−2601

Notes

The authors declare no competing financial interest.

REFERENCES

(1) Niyommaneerat, W.; Suwanteep, K.; Chavalparit, O. Sustainability indicators to achieve a circular economy: A case study of renewable energy and plastic waste recycling corporate social responsibility (CSR) projects in Thailand. *Journal of Cleaner Production* **2023**, *391*, No. 136203.

(2) Smorokov, A.; Kantaev, A.; Bryankin, D.; Miklashevich, A.; Kamarou, M.; Romanovski, V. Low-temperature method for desiliconization of polymetallic slags by ammonium bifluoride solution. *Environmental Science and Pollution Research* **2023**, *30* (11), 30271−30280.

(3) Smorokov, A.; Kantaev, A.; Bryankin, D.; Miklashevich, A.; Kamarou, M.; Romanovski, V. A novel low-energy approach to leucoxene concentrate desiliconization by ammonium bifluoride solutions. *Journal of Chemical Technology & Biotechnology* **2023**, *98* (3), 726−733.

(4) Smorokov, A.; Kantaev, A.; Bryankin, D.; Miklashevich, A.; Kamarou, M.; Romanovski, V. Low-temperature desiliconization of activated zircon concentrate by NH4HF2 solution. *Minerals Engineering* **2022**, *189*, No. 107909.

(5) Wang, H.; Wang, Y.; Liu, Z.; Luo, S.; Romanovski, V.; Huang, X.; Czech, B.; Sun, H.; Li, T. Rational construction of micron-sized zero-valent iron/graphene composite for enhanced Cr(VI) removal from aqueous solution. *Journal of Environmental Chemical Engineering.* **2022**, *10* (6), No. 109004.

(6) Zhou, Z.; Zhang, L.; Yan, B.; Wu, J.; Kong, D.; Romanovski, V.; Ivanets, A.; Li, H.; Chu, S.; Su, X. Removal of chromium from electroplating sludge by roasting-acid leaching and catalytic degradation of antibiotics by its residue. *Journal of Environmental Chemical Engineering.* **2024**, *12* (1), No. 111754.

(7) Romanovski, V.; Romanovskaia, E.; Moskovskikh, D.; Kuskov, K.; Likhavitski, V.; Arslan, M. F.; Beloshapkin, S.; Matsukevich, I.; Khort, A. Recycling of iron-rich sediment for surface modification of filters for underground water deironing. *Journal of Environmental Chemical Engineering.* **2021**, *9* (4), No. 105712.

(8) Romanovski, V.; Klyndyuk, A.; Kamarou, M. Green Approach for Low-energy Direct Synthesis of Anhydrite from Industrial Wastes of Lime Mud and Spent Sulfuric Acid. *Journal of Environmental Chemical Engineering.* **2021**, *9* (6), No. 106711.

(9) Romanovski, V.; Su, X.; Zhang, L.; Paspelau, A.; Smorokov, A.; Sehat, A. A.; Akinwande, A. A.; Korob, N.; Kamarou, M. Approaches for filtrate utilization from synthetic gypsum production. *Environmental Science and Pollution Research* **2023**, *30* (12), 33243−33252.

(10) Ferella, F.; Innocenzi, V.; Maggiore, F. Oil refining spent catalysts: A review of possible recycling technologies. *Resources, Conservation and Recycling* **2016**, *108*, 10−20.

(11) Alonso-Farinas, B.; Rodriguez-Galan, M.; Arenas, C.; Arroyo Torralvo, F.; Leiva, C. Sustainable management of spent fluid catalytic cracking catalyst from a circular economy approach. *Waste Management* **2020**, *110*, 10−19.

(12) Mouna, H. M.; Baral, S. S. A bio-hydrometallurgical approach towards leaching of lanthanum from the spent fluid catalytic cracking catalyst using Aspergillus niger. *Hydrometallurgy* **2019**, *184*, 175−182.

(13) Weng, Z.; Jowitt, S. M.; Mudd, G. M.; Haque, N. A detailed assessment of global rare earth element resources: opportunities and challenges. *Economic Geology* **2015**, *110* (8), 1925−1952.

(14) Pak, S. J.; Seo, I.; Lee, K. Y.; Hyeong, K. Rare earth elements and other critical metals in deep seabed mineral deposits: Composition and implications for resource potential. *Minerals* **2019**, *9* (1), 3.

(15) Yuksekdag, A.; Kose-Mutlu, B.; Zeytuncu-Gokoglu, B.; Kumral, M.; Wiesner, M. R.; Koyuncu, I. Process optimization for acidic leaching of rare earth elements (REE) from waste electrical and electronic equipment (WEEE). *Environmental Science and Pollution Research* **2022**, *29*, 7772−7781.

(16) Lin, P.; Yang, X.; Werner, J. M.; Honaker, R. Q. Application of Eh-pH diagrams on acid leaching systems for the recovery of REEs from bastnaesite, monazite and xenotime. *Metals* **2021**, *11* (5), 734.

(17) Battsengel, A.; Batnasan, A.; Narankhuu, A.; Haga, K.; Watanabe, Y.; Shibayama, A. Recovery of light and heavy rare earth elements from apatite ore using sulphuric acid leaching, solvent extraction and precipitation. *Hydrometallurgy* **2018**, *179*, 100−109.

(18) Banerjee, R.; Mohanty, A.; Chakravarty, S.; Chakladar, S.; Biswas, P. A single-step process to leach out rare earth elements from coal ash using organic carboxylic acids. *Hydrometallurgy* **2021**, *201*, No. 105575.

(19) Lazo, D. E.; Dyer, L. G.; Alorro, R. D.; Browner, R. Treatment of monazite by organic acids II: Rare earth dissolution and recovery. *Hydrometallurgy* **2018**, *179*, 94−99.

(20) Antonick, P. J.; Hu, Z.; Fujita, Y.; Reed, D. W.; Das, G.; Wu, L.; Shivaramaiah, R.; Kim, P.; Eslamimanesh, A.; Lencka, M.M.; Jiao, Y.; Anderko, A.; Navrotsky, A.; Riman, R. E. Bio-and mineral acid leaching of rare earth elements from synthetic phosphogypsum. *J. Chem. Thermodyn.* **2019**, *132*, 491−496.

(21) Mowafy, A. M. Biological leaching of rare earth elements. *World Journal of Microbiology and Biotechnology* **2020**, *36* (4), 61.

(22) Mouna, H. M.; Baral, S.S. A bio-hydrometallurgical approach towards leaching of lanthanum from the spent fluid catalytic cracking catalyst using Aspergillus niger. *Hydrometallurgy* **2019**, *184*, 175−182.

(23) Zhao, Z.; Qiu, Z.; Yang, J.; Lu, S.; Cao, L.; Zhang, W.; Xu, Y. Recovery of rare earth elements from spent fluid catalytic cracking catalysts using leaching and solvent extraction techniques. *Hydrometallurgy* **2017**, *167*, 183−188.

(24) Lu, G.; Lu, X.; Liu, P. Recovery of rare earth elements from spent fluid catalytic cracking catalyst using hydrogen peroxide as a reductant. *Minerals Engineering* **2020**, *145*, No. 106104.

(25) Sadeghi, S. M., Jesus, J., Pinto, E., Almeida, A., Soares, H. A Simple and Flexible Flowsheet Process for Efficient and Selective Metal Recycling from Spent Fluid Cracking Catalysts. *16th International Conference on Environmental Science and Technology*, Rhodes, Greece, 4−7 September 2019. https://www.semanticscholar.org/paper/A-Simple-and-Flexible-Flowsheet-Process-for-and/b9690d72d85a68c6a8d28e46c40333cdc8fda52e.

(26) Sadeghi, S. M.; Jesus, J.; Pinto, E.; Almeida, A. A.; Soares, H. M. A simple, efficient and selective process for recycling La (and Al) from fluid cracking catalysts using an environmentally friendly strategy. *Minerals Engineering* **2020**, *156*, No. 106375.

(27) Maidel, M.; de Santana Ponte, M. J. J.; de Araújo Ponte, H. Recycling lanthanum from effluents of elektrokinetic treatment of FCC spent catalyst, using a selective precipitation technique. *Sep. Purif. Technol.* **2019**, *210*, 251−257.

(28) Alcaraz, L.; Largo, O. R.; Alguacil, F. J.; Montes, M. Á.; Baudín, C.; López, F. A. Extraction of lanthanum oxide from different spent fluid catalytic cracking catalysts by nitric acid leaching and Cyanex 923 solvent extraction methods. *Metals* **2022**, *12* (3), 378.

(29) Martsul', V.N.; Kozlowskaya, I.Y. Recovery of lanthanum from acid leaching solutions of spent cracking catalyst. *Russian Journal of Applied Chemistry* **2015**, *88*, 1589−1593.

(30) Ward, J. W. A spectroscopic study of the surface of zeolite Y: the adsorption of pyridine. *J. Colloid Interface Sci.* **1968**, *28* (2), 269−278.

(31) Thommes, M.; Kaneko, K.; Neimark, A. V.; Olivier, J. P.; Rodriguez-Reinoso, F.; Rouquerol, J.; Sing, K. S. Physisorption of gases, with special reference to the evaluation of surface area and pore size distribution (IUPAC Technical Report). *Pure and Applied Chemistry* **2015**, *87* (9-10), 1051−1069.

(32) Rare and scattered elements. In *Chemistry and technology: in 3 books: textbook for universities*; Korovin, S. S., Ed.; MISIS: Moscow, 1996; pp 376. https://www.studmed.ru/korovin-ss-red-redkie-i-rasseyannye-elementy-himiya-i-tehnologiya-kniga-2_d4f3cf0719b.html.

(33) Redaoui, D.; Sahnoune, F.; Heraiz, M.; Raghdi, A. Mechanism and kinetic parameters of the thermal decomposition of gibbsite

https://doi.org/10.1021/acssusresmgt.4c00364
ACS Sustainable Resour. Manage. 2024, 1, 2593−2601

Al(OH)3 by thermogravimetric analysis. *Acta Physica Polonica A* **2017**, *131* (3), 562−565.
(34) Taspinar, E.; Tas, A. C. Low-temperature chemical synthesis of lanthanum monoaluminate. *Journal of the American Ceramic Society* **1997**, *80* (1), 133−141.
(35) Sim, Y.; Yang, I.; Kwon, D.; Ha, J. M.; Jung, J. C. Preparation of LaAlO3 perovskite catalysts by simple solid-state method for oxidative coupling of methane. *Catalysis Today* **2020**, *352*, 134−139.
(36) Boronat, C.; Rivera, T.; García-Guinea, J.; Correcher, V. Cathodoluminescence emission of REE (Dy, Pr and Eu) doped LaAlO3 phosphors. *Radiation Physics and Chemistry* **2017**, *130*, 236−242.
(37) Bespalko, Y.; Kuznetsova, T.; Kriger, T.; Chesalov, Y.; Lapina, O.; Ishchenko, A.; Larina, T.; Sadykov, V.; Stathopoulos, V. La2Zr2O7/LaAlO3 composite prepared by mixing precipitated precursors: Evolution of its structure under sintering. *Materials Chemistry and Physics* **2020**, *251*, No. 123093.
(38) Patnaik, P. *Handbook of inorganic chemicals*, Vol. *529*; McGraw-Hill: New York, 2003; pp 769−771.
(39) Mouna, H. M.; Baral, S. S.; Mohapatra, P. Leaching of metals from spent fluid catalytic cracking catalyst using acidothiobacillus ferrooxidans and comparing its leaching efficiency with organic and inorganic acids. *Journal of Environmental Chemical Engineering* **2021**, *9* (5), No. 105522.
(40) Muddanna, M. H.; Baral, S. S. A comparative study of the extraction of metals from the spent fluid catalytic cracking catalyst using chemical leaching and bioleaching by Aspergillus niger. *Journal of Environmental Chemical Engineering* **2019**, *7* (5), No. 103335.
(41) Muddanna, M. H.; Baral, S. S. Bioleaching of rare earth elements from spent fluid catalytic cracking catalyst using Acidothiobacillus ferrooxidans. *Journal of Environmental Chemical Engineering* **2021**, *9* (1), No. 104848.
(42) Muddanna, M. H.; Baral, S. S. Leaching of nickel and vanadium from the spent fluid catalytic cracking catalyst by reconnoitering the potential of Aspergillus niger associating with chemical leaching. *Journal of Environmental Chemical Engineering* **2019**, *7* (2), No. 103025.
(43) Mouna, H. M.; Baral, S. S. A bio-hydrometallurgical approach towards leaching of lanthanum from the spent fluid catalytic cracking catalyst using Aspergillus niger. *Hydrometallurgy* **2019**, *184*, 175−182.
(44) Chadha, P.; Yadav, P.; Sharma, M.; Sharma, Y.; Nangia, R.; Sharma, K.; Maksudovna, V.K. Global trends in waste materials: A bibliometric analysis. *Materials Today: Proceedings.* **2023**.
(45) Vafaeva, K.M.; Chhetri, A.; Sudan, P.; Mishra, M.; Babu, B.S.; Mongal, B.N. Polymer Matrix Nanocomposites for Sustainable Packaging: A Green Approach. *E3S Web of Conferences* **2024**, *537*, 08001.
(46) Vafaeva, K. M.; Karpov, D. F.; Pavlov, M. V.; Srinivas, N.; Goyal, W.; Negi, G. S.; Sobti, S.; Soujnya, R.; Tiwari, D. K. Enhancing Energy Efficiency in Greenhouses: Gas-Radiant Heating with Preheated Ventilation. *E3S Web of Conferences* **2024**, *581*, 01042.
(47) Karpov, D.; Dyudina, O.; Pavlov, M. A review on modern heat-insulating materials for improving the energy efficiency of buildings and life-support utilities. *E3S Web of Conferences* **2021**, *288*, 01099.
(48) Pavlov, M. V.; Karpov, D. F. Solution of the boundary value problem of heat and mass transfer by the method of joint application of the integral Laplace transform and the Bubnov-Galerkin variational method for conditions of radiant soil heating. *Prirodoobustrojstvo* **2024**, No. 3, 31−36.
(49) Nuriev, M.; Zaripova, R.; Yanova, O.; Koshkina, I.; Chupaev, A. Enhancing MongoDB query performance through index optimization. *E3S Web of Conferences* **2024**, *531*, 03022.
(50) Viktorov, I.; Gibadullin, R. The principles of building a machine-learning-based service for converting sequential code into parallel code. *E3S Web of Conferences* **2023**, *431*, 05012.
(51) Mary Ealias, A.; Meda, G.; Tanzil, K. Recent progress in sustainable treatment technologies for the removal of emerging contaminants from wastewater: A review on occurrence, global status and impact on biota. *Reviews of Environmental Contamination and Toxicology* **2024**, *262* (1), 16.

https://doi.org/10.1021/acssusresmgt.4c00364
ACS Sustainable Resour. Manage. 2024, 1, 2593−2601